RESEARCH PAPER

MICHAEL ADDITION REACTION KINETICS OF ACETOACETATES AND ACRYLATES FOR THE FORMATION OF POLYMERIC NETWORKS

Sharlene R. Williams[a], Kevin M. Miller[b] and Timothy E. Long[a]*

[a]*Department of Chemistry, Macromolecules and Interfaces Institute, Virginia Tech, Blacksburg, VA 24061-0344, USA*

[b]*Rohm and Haas Company, Spring House, PA 19477, USA*

*E-mail: telong@vt.edu

Contents

ABSTRACT

2-Ethylhexyl acrylate and ethyl acetoacetate were reacted in a Carbon – Michael addition reaction as a model for subsequent studies of polymer networks. A statistical design of reactions was conducted in the presence of an *in-situ* ATR FTIR spectrometer to determine the effect of solvent, base, base concentration, and reactant stoichiometry on the observed rate constant. In particular, a central composite statistical design of experiments analysis was performed for model reactions that were catalyzed using either 1,8-diazbicyclo[5.4.0]undec-7-ene (DBU) or K_2CO_3 at various concentrations. Poly(propylene glycol) bisacetoacetate (PPG BisAcAc) and poly(propylene glycol) diacrylate (PPGDA) networks were then prepared in the absence of solvent at 23°C based on optimized conditions in the presence of DBU and K_2CO_3. In a similar fashion to model studies, *in-situ* FTIR spectroscopy was utilized, and observed rate constants were determined. The influence of PPG BisAcAc molecular weight on dynamic mechanical properties was determined and gel fraction analysis was conducted. It appears that the selection of base significantly altered the rate of the reaction, but had an insignificant effect on mechanical properties.

KEYWORDS: Michael addition, solvent effects, base effects, design of experiments, *in-situ* FTIR

1. INTRODUCTION

The Michael reaction, which was discovered by Arthur Michael in the late 1800s, is an efficient and versatile reaction. The Carbon – Michael addition reaction has received significant attention in recent literature for the preparation of novel polymers and composites [1 – 11]. The Michael reaction typically refers to the base-catalyzed addition of an enolate anion (Michael donor) to an activated α,β-unsaturated carbonyl-containing compound (Michael acceptor) [5 – 8]. One of the best-known Carbon – Michael transformations is the base-catalyzed addition of ethyl acetoacetate to methyl acrylate [12]. The mechanism of the reaction is relatively straightforward, and every step is in equilibrium and thermodynamically dependent on the relative strength of the base and the type of acetoacetate. The acetoacetate is first deprotonated with a base, which provides an enolate anion in equilibrium. The enolate anion then reacts in a 1,4-conjugate addition to the alkene group of the methyl acrylate. The carbonyl of the acrylate stabilizes

the resulting anion until proton transfer occurs, which regenerates the base. The overall driving force for the conjugate addition is the replacement of a π bond with a σ bond. Thus, there is a preference for 1,4-addition rather than 1,2-addition. However, in some cases, kinetically controlled reaction conditions afford attack at the carbonyl carbon rather than at the β-carbon of the alkene [13].
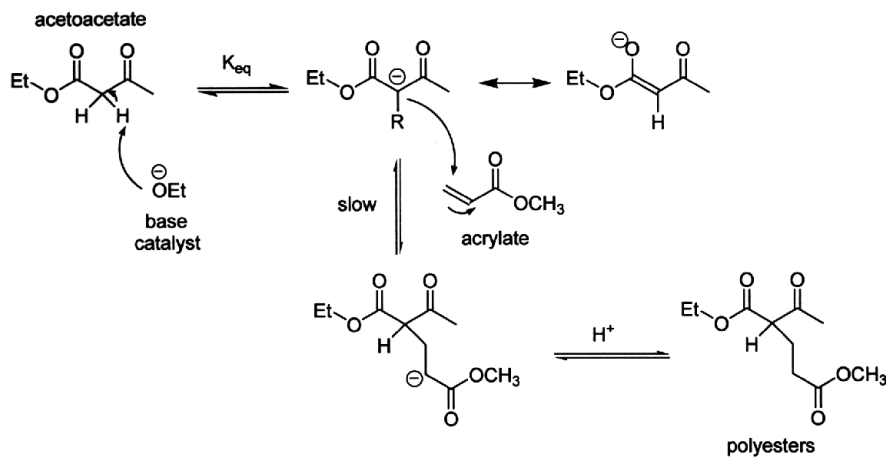
**Scheme 1**   General Carbon – Michael reaction.

From the above reaction scheme, one can observe that the rate-determining step is the attack of the enolate anion on the activated alkene. The reaction rate is therefore second order overall with respect to the enolate anion and the alkene acceptor. The concentration of the enolate is a function of the base strength and the K_{eq} of the deprotonation step of the active methylene hydrogen. It follows that the equilibrium constant is dependent on the relative strength of the base and the structure of the acetoacetate.

It is worthy to note that the product of the first Michael addition has one remaining active methylene hydrogen which can be deprotonated and thus undergo a second addition to another acrylate (Scheme 2). Clemens *et al.* has documented that the second pK_a is expected to have a value of 13 (versus the pK_a of the initial active hydrogen of 12) [14]. The second deprotonation therefore has a different equilibrium constant (K_{eq}) and it is assumed that the concentration of the first Michael adduct will be low. As a result, the concentration of the enolate at any rate (especially in the early stages of the reaction) is not affected by this secondary reaction.
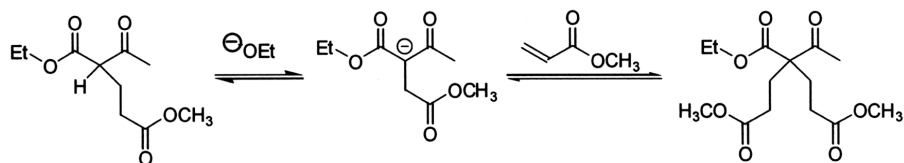
Scheme 2 Second Michael addition.

It follows that a rate law can be determined for the above reaction sequence. Writing the reactions in terms of the Michael addition, the following reaction sequences are obtained:
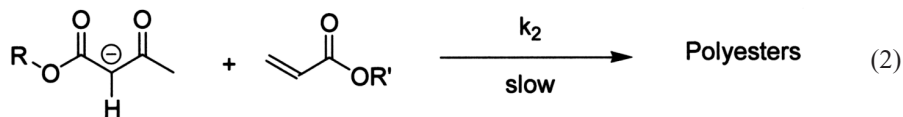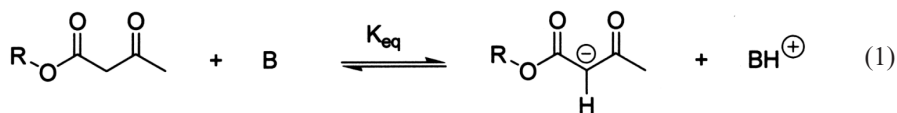
The subsequent rate equations based on the reaction sequence are the following:

$$K_{eq} = [AcAc^-][BH^+]/[AcAc][B] \tag{3}$$

$$\text{Rate} = k_2[AcAc^-][\text{Acrylate}] = k_2 K_{eq}([B]/[BH^+])[AcAc][\text{Acrylate}] \tag{4}$$

The choice of catalyst has a tremendous effect on the reaction kinetics. As previously noted, the concentration of the enolate and therefore the value of K_{eq} is highly dependent on the relative base strength. In the case of strong bases, K_{eq} will lie to the right and the concentration of the enolate anion is approximately equal to the concentration of the base (achieving a steady state concentration). The resulting rate law follows pseudo first-order kinetics [Eqn (5)]. In this rate expression, there is a pseudo first-order dependence on acrylate concentration, where k_{obs} is a function of base concentration.

$$\text{Rate} = k_{obs}[\text{Acrylate}] \tag{5}$$

In the case of weaker base catalysts, K_{eq} has a moderate value, but is not large. This introduces the equilibrium constant into the rate law and results in the reaction following second order kinetics [Eqn (4)]. Clemens *et al*. has completed an extensive study on how base strength affects reaction kinetics and molecular

weight when the Michael addition is used to prepare crosslinked acetoacetate resins for thermoset coatings [14]. In their model study, Clemens *et al.* analyzed the efficacy of weaker bases such as tetramethylguanidine (TMG), triethylamine (TEA), 1,8-diazabicyclo[5.4.0]undec-7-ene (DBU), and 1,5-diazabicyclo[4.3.0]non-5-ene (DBN) and found that, as indicated by Eqn (4), the rate of the reaction is dependent on catalyst concentration. In the cases of stronger bases such as hydroxide ion, a steady-state concentration of enolate anion is achieved and pseudo-first order kinetics are observed [Eqn (5)].

Our current research seeks to understand fundamentally the kinetics of the Michael reaction with both homogeneous and heterogeneous catalysts. Model reactions as described herein allowed us to understand the kinetics of the Michael reaction as a function of acrylate to acetoacetate molar ratio, base concentration, and solvent. We subsequently applied our understanding of the model reactions to the formation of polymeric networks containing poly(propylene glycol) (PPG). The kinetics of the network formation as well as dynamic mechanical analysis of the networks are described.

2. EXPERIMENTAL

2.1 Materials and procedures

tert-Butyl acetoacetate (tBuAcAc, 98%), 800 g/mol poly(propylene glycol) diacrylate (PPGDA), ethyl acetoacetate (EtAcAc, 99%), and 1,8-diazbicyclo[5.4.0]undec-7-ene (DBU, 98%) were purchased from Aldrich and used as received. 2-Ethylhexyl acrylate (EHA, 98%) was purchased from Aldrich, and the inhibitors were removed by passing the as received EHA through a column of alumina. Tetrahydrofuran (THF, EMD Science, HPLC grade), ethanol (Aldrich, anhydrous, $\geqslant$ 99.5%), *m*-xylene (Aldrich, anhydrous, 99 + %), and dimethylsulfoxide (DMSO, Aldrich, anhydrous, $\geqslant$ 99.5%) were used as received. Finely ground potassium carbonate (K_2CO_3) and poly(propylene glycol) bisacetoacetate (PPG BisAcAc) oligomers of 2000, 4000, and 8000 g/mol were kindly supplied by Rohm and Haas, the synthesis of which has been previously described [3,15]. All ARCOL® and ACCLAIM® polyols were kindly supplied by Bayer Co. PPG BisAcAc of 1000 g/mol was prepared from ARCOL® poly(propylene glycol) diol. PPG BisAcAc oligomers of 2000, 4000, and 8000 g/mol were prepared from ACCLAIM® poly(propylene glycol) diols, using a method described previously and described below [3,15].

In a typical procedure, Arcol® PPG (10.0 g, 10 mmol) and tBuAcAc (6.3 g, 40 mmol, 4 equiv.) were charged to a two-necked 100-ml flask, equipped with a short-path distillation head, receiving flask, and magnetic stirrer. The mixture was maintained at 150°C for 3 h and vacuum (0.1 mmHg) was applied to remove the *tert*-butanol by-product and excess tBuAcAc. An additional 6.3 g tBuAcAc was added and heating continued for 3 h at 150°C in order to ensure quantitative functionalization. Vacuum (0.1 mmHg) at 150°C was applied to remove volatile starting reagents and reaction by-products. ^{1}H NMR spectroscopy of the PPG BisAcAc oligomers confirmed the desired composition. ^{1}H NMR (400 MHz, CDCl$_3$) of the 1000 g/mol PPG BisAcAc: $\delta = 1.12$ ppm (br, PPG CH_3), 1.24 ppm (dd, 6H, CHCH_3OAcAc), 2.26 ppm (s, 6H,COCH_2COCH_3), 3.4 ppm (br, PPG CH), 3.6 ppm (br, PPG CH_2), 5.08 ppm (m, 4H, CH_2CHCH$_3$OAcAc), 5.29 ppm (s, enol C=CH—C=O).

2.2 *In-situ* FTIR reactions for model studies

A typical reaction mixture consisted of a 1.4 : 1 mol ratio of acrylate to acetoacetate and 3 mol% 1,8-diazabicyclo-[5.4.0]-undec-7-ene (DBU) as the base in the presence of the *in-situ* FTIR spectrometer. The *in-situ* FTIR ATR probe was cleaned with THF prior to running a background scan in air. A three-necked, round-bottomed flask that was equipped with a stir bar was charged with 6.000 g (0.04610 mol) ethyl acetoacetate, and 11.895 g (0.06455 mol) 2-ethylhexyl acrylate was weighed in a separate vial. The round-bottomed flask and vial were placed in a 35°C oil bath. DBU (3 mol%, 511 µl) was added to the round-bottomed flask, and the contents were allowed to equilibrate for 60 min. After the 60 min pre-equilibration, the reaction was monitored with the *in-situ* FTIR spectrometer. Once the first scan was complete, the acrylate was quickly added to the round-bottomed flask. For the reactions with solvent, the reaction flask was diluted 50% with THF by weight.

2.3 ^{1}H NMR spectroscopic kinetic studies

For the reactions completed in solvent, ^{1}H NMR spectroscopy was also used to determine relative rates of reaction. In a typical procedure, ethyl acetoacetate (5.00 g, 0.038 mol), diluted 50% w/w with 5.00 g solvent (THF, DMSO, EtOH, *m*-xylene), was warmed to 35°C using an oil bath. Once the mixture was at 35°C, 1 mol% potassium carbonate was added and the mixture allowed to stir for 30

minutes. Butyl acrylate (4.93 g, 0.038 mol), pre-warmed to 35°C, was added, and loss of the acrylate signal was monitored by ^{1}H NMR over time. Plots of ln[acrylate] versus time resulted in a linear fit ($r^2 > 0.998$) of which the slope was the observed pseudo-first order rate constant. Analysis of the post-reaction products resulted in $>99:1$ ratio of the mono to bis Carbon–Michael substitution products.

2.4 Statistical design of experiments

A central composite statistical design of experiments (DOE) was developed for the investigation of the kinetics of the Michael reaction. The constants for the DOE included stir rate, reaction temperature (35°C), air atmosphere, and an acetoacetate with base pre-equilibration time (1 h). The factors for the DOE included the EHA:EtAcAc molar ratio, choice of basic catalyst, catalyst concentration, and the presence or absence of solvent. Specifically, the EHA:EtAcAc molar ratio ranged from 0.8 to 2.0, the choice of basic catalyst was DBU or K_2CO_3, the catalyst concentration ranged from 1 to 5 mol%, and the solvent was THF or bulk. The observed rate constant was the response modelled for the DOE. Stat-Ease software Design-Expert version 6.0.1 was used, and the DOE experimental design is given in Table 1.

Table 1 DOE design

Std	Run	Factor 1: Acrylate Molar Ratio (relative to AcAc)	Factor 2: Base Concentration (mol%)	Factor 3: Solvent
2	1	1.4 : 1.0	3.0	Bulk
11	2	0.8 : 1.0	1.0	Bulk
17	3	2.0 : 1.0	1.0	THF
9	4	2.0 : 1.0	5.0	THF
1	5	1.4 : 1.0	3.0	THF
14	6	2.0 : 1.0	1.0	Bulk
6	7	0.8 : 1.0	1.0	THF
8	8	2.0 : 1.0	3.0	Bulk
15	9	1.4 : 1.0	1.0	Bulk
7	10	1.4 : 1.0	5.0	THF
16	11	0.8 : 1.0	3.0	Bulk
12	12	0.8 : 1.0	5.0	THF
18	13	2.0 : 1.0	3.0	THF
5	14	1.4 : 1.0	5.0	Bulk
10	15	2.0 : 1.0	5.0	Bulk
3	16	0.8 : 1.0	3.0	THF
13	17	0.8 : 1.0	5.0	Bulk
4	18	1.4 : 1.0	1.0	THF

2.5 Network formation

2000 g/mol PPG BisAcAc (0.75 g, 3.75×10^{-4} mol) and PPGDA (0.42 g, 5.25×10^{-4} mol, 1.4 equiv) were mixed thoroughly to form a clear, homogeneous liquid. DBU catalyst was quickly added and mixed thoroughly. The mixture was then transferred to a Teflon® mould and was allowed to cross-link for 24 h at room temperature. The resulting films were dried at reduced pressure (0.1 mm Hg) for 18 h at room temperature. Similar preparations were used to form all Carbon–Michael networks described in this manuscript, with the exception that K_2CO_3 was substituted for DBU.

2.6 Characterization

^{1}H NMR spectroscopy was utilized to determine the PPG BisAcAc oligomer composition, number average molecular weight, percent functionalization, and to confirm Michael reactions. A 400 MHz Varian UNITY spectrometer was used to characterize the oligomers and polymerizations in $CDCl_3$ at 23°C. Dynamic mechanical analysis (DMA) was conducted on a TA Instruments Q800 dynamic mechanical analyzer in tension mode at a frequency of 1 Hz, an oscillatory amplitude of 15 µm, and a static force of 0.01 N. The temperature ramp was 3°C/min. The glass transition temperature (T_g) was determined from the storage modulus curves. The resulting networks were characterized for gel fraction via Soxhlet extractions in THF for 3 h and subsequently dried in an oven at reduced pressure (0.1 mmHg) at 60°C for 18 h, or until constant weight was observed. The gel fraction was determined by dividing the initial mass (m_i) with the final mass (m_f). Rheological experiments were conducted on a TA Instruments AR2000 Rheometer at a frequency of 1 Hz and a temperature of 25°C. The gel time was recorded when the storage modulus (G') and loss modulus (G'') were equal.

3. RESULTS AND DISCUSSION

3.1 Model reactions with EtAcAc and EHA

The kinetics of the Michael reaction were analyzed using an *in-situ* FTIR spectrometer and DOE software. During the *in-situ* FTIR reactions, the disappearance of the vinyl CH_2 out-of-plane wag frequency was monitored at 810 cm^{-1}. Scheme 3 depicts the reaction strategy.
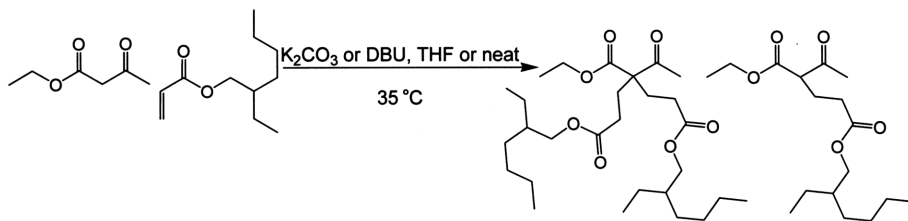
Scheme 3 Model reactions of EtAcAc and EHA.

A waterfall plot, which shows the *in-situ* FTIR absorbance as a function of time, is shown in Figure 1 for a reaction of EtAcAc and EHA with a 1.4 : 1.0 acrylate to AcAc molar ratio, 3 mol% K_2CO_3, in THF. As demonstrated by the FTIR data, this reaction was complete within 1 h. A 2-dimensional plot also reveals the disappearance of the vinyl CH_2 out-of-plane wag mode, with the peak decreasing in intensity as the reaction proceeded (Figure 2).

To further confirm that the vinyl groups of EHA were consumed during the reaction, samples were removed from a Michael reaction of EHA and EtAcAc and quenched with 0.65 M trifluoroacetic acid in $CDCl_3$. As demonstrated in Figure 3, the acrylate protons are consumed over time, and after 1 h, the acrylate is quantitatively consumed.
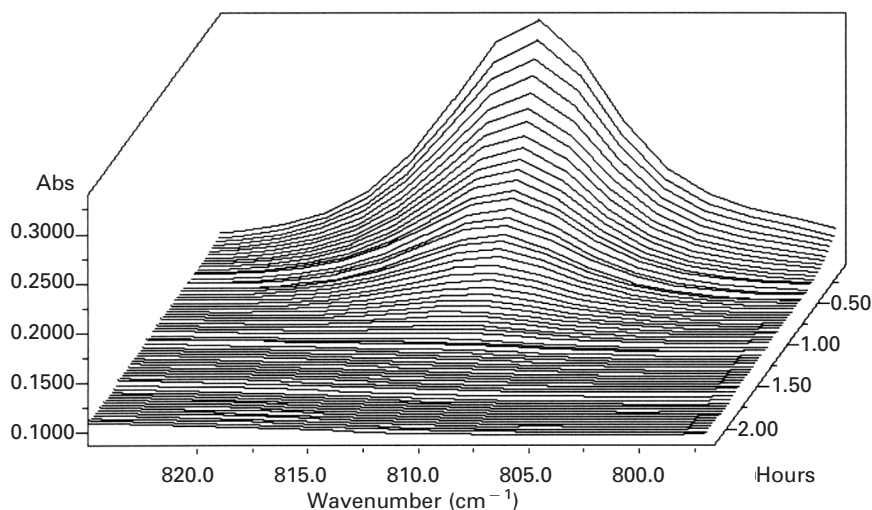

Figure 1 *In-situ* FTIR spectra of EtAcAc and EHA Michael reaction, waterfall plot: 1.4 : 1.0 acrylate to AcAc, 3 mol% K_2CO_3, in THF.
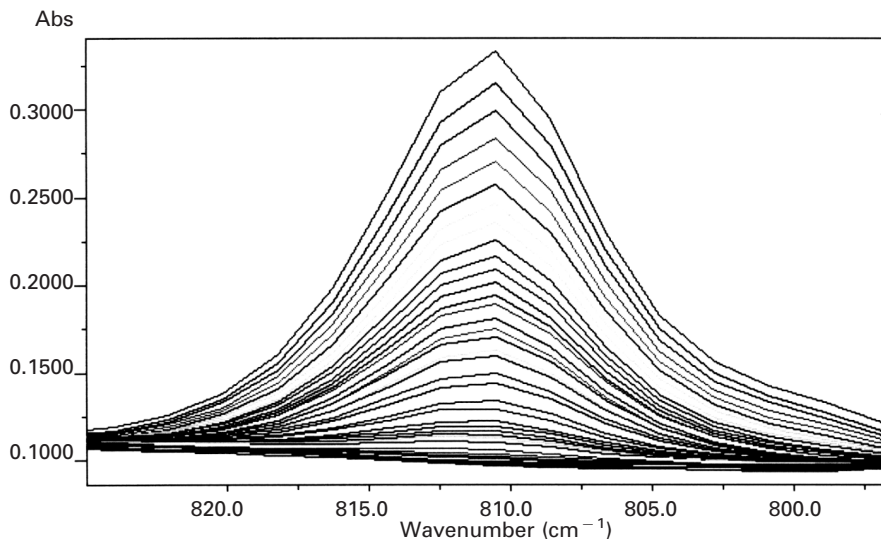
Figure 2 *In-situ* FTIR spectra of EtAcAc and EHA Michael reaction 2D plot: 1.4:1.0 acrylate to AcAc, 3 mol% K_2CO_3, in THF.

In the following section, three areas of interest are investigated with respect to the kinetics of the Carbon–Michael reaction, *i.e.*, base concentration, solvent effects, and acrylate concentration. The goal is to provide a fundamental
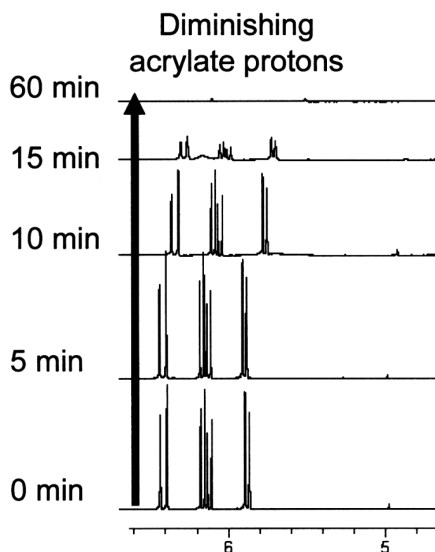

Figure 3 Stacked ^{1}H NMR spectra of EHA and EtAcAc Michael reaction versus time.

understanding of the reaction kinetics which may provide some help in under-standing the kinetics of formation and mechanical properties of the corresponding polymer networks.

3.2 Effect of base concentration

As shown in Table 1, a series of reactions were performed, with various base concentrations and acrylate to acetoacetate molar ratios. Furthermore, the base was varied either as ground K_2CO_3 or DBU, and the reaction was performed in either THF solvent or in the absence of solvent. The vinyl CH_2 out-of-plane wag frequency was monitored over time and compared to a baseline for every experiment. From this, the pseudo-first order plots were constructed and the observed rate constants were calculated from the slopes of the linear fits. The effect of DBU concentration is depicted in Figure 4. As the base concentration was increased from 1 to 5 mol%, there was a systematic increase in the observed rate constant. Observed rate constants of 4.20×10^{-4}, 8.30×10^{-4}, and $2.00 \times 10^{-3}\,s^{-1}$ for 1, 3, and 5 mol% DBU, respectively, were calculated.
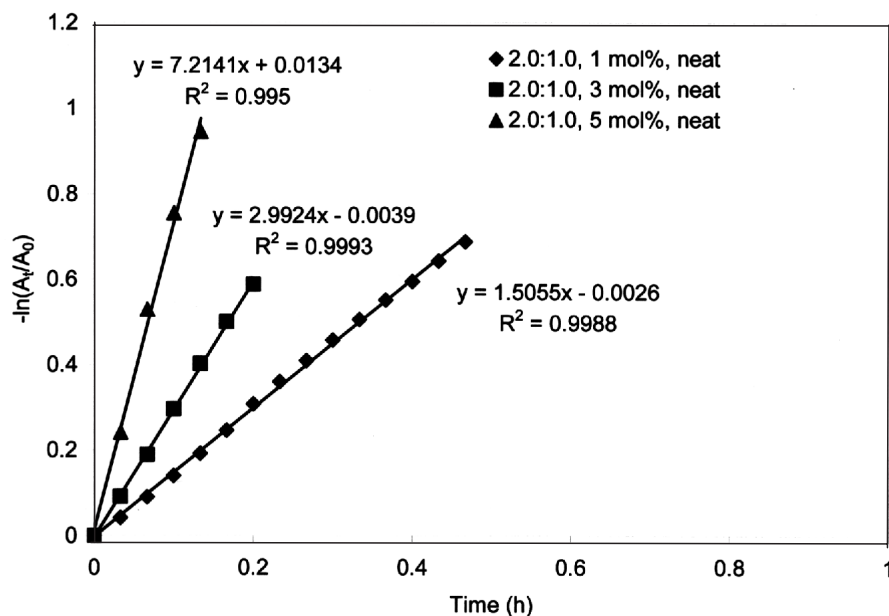

Figure 4   The effect of base concentration on rate constant for the EtAcAc and EHA Michael reaction in the presence of DBU. Reaction conditions: 2.0 : 1.0 mol ratio acrylate to AcAc, 35°C, neat, DBU.

Similar experiments were conducted with K_2CO_3 as the basic catalyst in the model Michael reactions. The effect of K_2CO_3 concentration is depicted in Figure 5. As expected, when the base concentration is increased from 1 to 5 mol%, there was a systematic increase in the slopes, and thus an increase in the observed rate constant. Observed rate constants of 2.90×10^{-4}, 2.43×10^{-3}, and $4.6 \times 10^{-3}\,s^{-1}$ for 1, 3, and 5 mol% K_2CO_3, respectively, were calculated.

3.3 Effect of solvent on Carbon–Michael reactions

3.3.1 *Effect of solvent using* in-situ *FTIR*

Typical Carbon–Michael reaction solvents include methanol, ethanol, diethyl ether, tetrahydrofuran, benzene, xylene, dioxane, and mixtures of these solvents. Initially, protic solvents were desirable in the Carbon–Michael reaction to promote rapid proton transfer; however, Schlessinger *et al*. have shown that high yielding reactions could also be achieved using aprotic solvents [16,17]. The choice of solvent strongly depends on the solubility of the catalyst, donor, and acceptor as well as sensitivity to side reactions. For example, if the reactants or
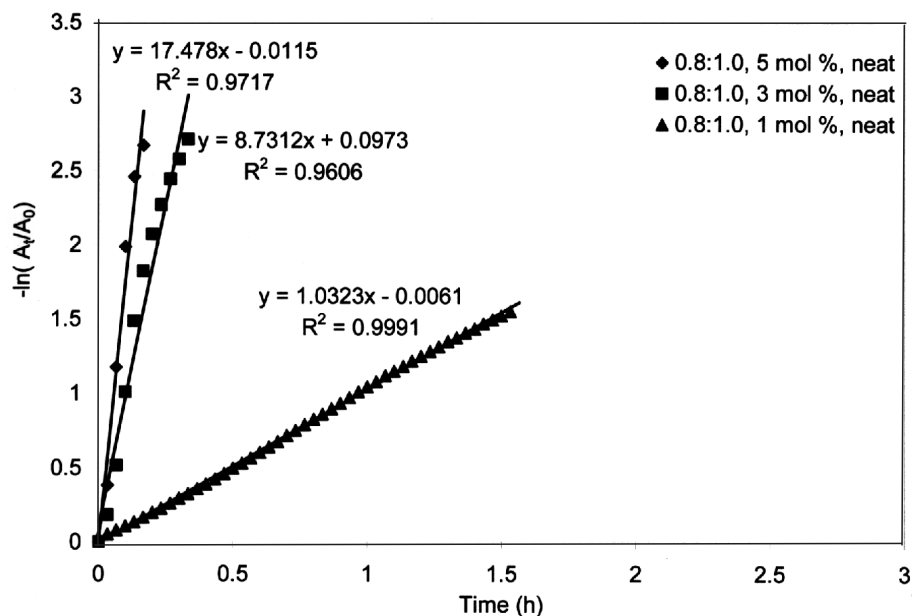

Figure 5 The effect of base concentration on rate constant for EtAcAc and EHA Michael reaction in the presence of K_2CO_3. Reaction conditions: 0.8 : 1.0 mol ratio acrylate to AcAc, 35°C, neat, K_2CO_3.
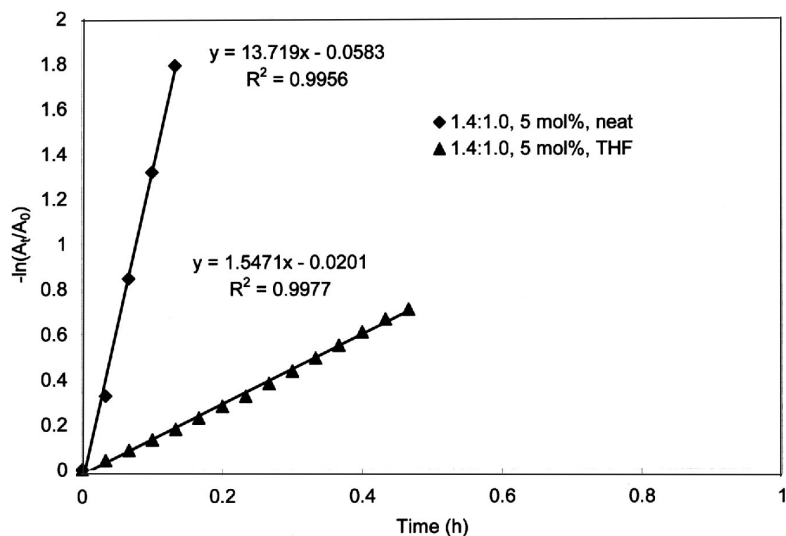
Figure 6 The effect of solvent on rate constant for the EtAcAc and EHA Michael reaction in the presence of DBU. Reaction conditions: $1.4:1.0$ mol ratio acrylate to AcAc, 5 mol% catalyst, 35°C, DBU.

products are susceptible to alcoholysis (ester exchange or hydrolysis), self-condensation of the substrate, or the 'retro-Michael' reaction, then a non-hydroxylic solvent should be chosen [18]. Reactions can even be run without solvent utilizing bases such as sodium amide.
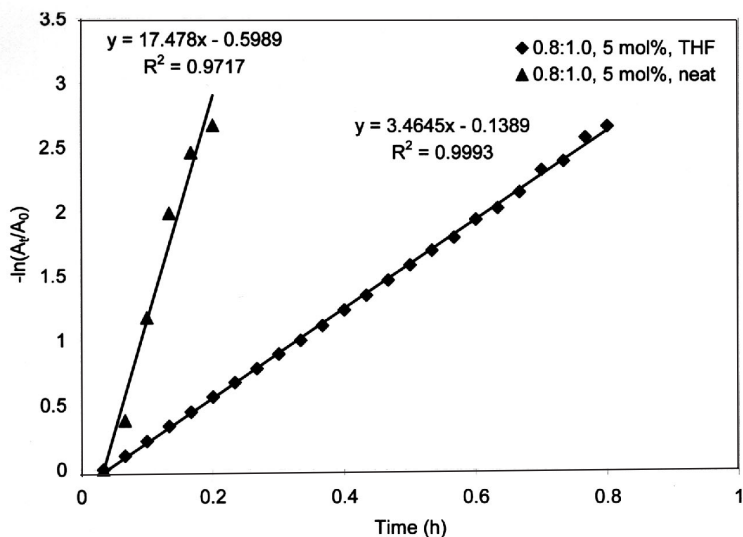

Figure 7 The effect of solvent on the rate constant for EtAcAc and EHA Michael reaction in the presence of K_2CO_3. Reaction conditions: $0.8:1.0$ mol ratio acrylate to AcAc, 5 mol% catalyst, 35°C, K_2CO_3.

As expected, the presence of solvent significantly influenced the observed rate constant in the reactions catalyzed by both DBU and potassium carbonate, as shown in Figures 6 and 7. The calculated observed rate constants were $3.70 \times 10^{-4}\,s^{-1}$ for the reaction conducted in THF, and $3.81 \times 10^{-3}\,s^{-1}$ for the reaction conducted without solvent. The presence of the relatively non-polar THF solvent leads to a decrease in reaction rate due to the lower dielectric constant ($DE = 7.6$ for THF) compared with the solvent-free system [19].

For the reactions catalyzed with K_2CO_3 (Figure 7), the calculated observed rate constants are $9.60 \times 10^{-4}\,s^{-1}$ for the reaction conducted in THF, and $4.86 \times 10^{-3}\,s^{-1}$ for the reaction conducted in the absence of solvent. As expected, the higher concentrations of functional groups lead to a more rapid reaction.

3.3.2 Effect of solvent using ^1H NMR

To validate the effects of THF solvent in the above *in-situ* FTIR studies, a similar study was conducted using ^1H NMR to determine reaction kinetics that covered a wider range of solvents. The same model reaction of EtAcAc and EHA was used, but at a 1 : 1 molar ratio. Two solvents of lower dielectric constant (*m*-xylene and THF) and two solvents of higher dielectric constant (ethanol and DMSO) were chosen [20]. From Table 2, a clear correlation was observed between solvent polarity and the value of k_{obs}. Note that when a solvent with a lower dielectric constant was used (*m*-xylene, THF), the observed reaction rate decreased compared to the solvent-free reaction. Both ethanol and DMSO provided a rate enhancement. The highly polar solvents stabilized the transition state(s) of the reaction, leading to lower activation energies and faster kinetics.

3.4 Effect of acrylate concentration on Carbon–Michael kinetics

Although a continued increase in starting acrylate concentration led to an increase in the bis Carbon–Michael product (and thus leading to more complex kinetics), it was of interest to investigate the effect of concentration

Table 2 Effect of solvent on k_{obs} – ^1H NMR method

Solvent	DE	k_{obs} (min^{-1})	Relative rate
THF	2.3	9.68×10^{-4}	0.08
m-Xylene	7.6	1.85×10^{-3}	0.16
No solvent	–	1.15×10^{-2}	1.00
Ethanol	24.5	2.85×10^{-2}	2.48
DMSO	78	1.86×10^{-1}	16.2

Table 3   Effect of acrylate : acetoacetate molar ratio on k_{obs}

Base	Acrylate : AcAc	k_{obs} (s^{-1})
DBU	0.8 : 1.0	4.58×10^{-3}
DBU	1.4 : 1.0	3.81×10^{-3}
DBU	2.0 : 1.0	2.00×10^{-3}
K_2CO_3	0.8 : 1.0	9.30×10^{-4}
K_2CO_3	1.4 : 1.0	1.14×10^{-3}
K_2CO_3	2.0 : 1.0	5.90×10^{-4}

changes on k_{obs}. Table 3 provides a summary of the *in-situ* FTIR data for observed rates of reaction when the acrylate : acetoacetate ratio was varied from 0.8 : 1.0 to 1.4 : 1.0 to 2.0 : 1.0. These reactions were completed without solvent in the presence of 5 mol% catalyst. There was no clear trend when the acrylate : a-cetoacetate ratio was at 1.4 : 1.0 or 2.0 : 1.0 since the fluctuations in acrylate concentration led to complex kinetics where the k_{obs} value reflects the reaction rates of both the first and second Carbon – Michael additions. However, the observed rates of reaction were always slowest for the reactions conducted with a 0.8 : 1.0 acrylate : acetoacetate ratio.

3.5 Design of experiment (DOE) analysis

Once all 36 experiments were conducted and observed rate constants were determined, a statistical analysis was conducted to determine the influence of each component on the observed rate constant. The statistical design software provided a model for the observed rate constant as a function of base concentration and acrylate to acetoacetate molar ratios. The equations in terms of these factors in the presence of DBU are:

$$
\begin{aligned}
\text{DBU THF } k_{obs} = {} & 3.63618 \times 10^{-4} - 1.28056 \times 10^{-4}*\text{Acrylate mol ratio} \\
& + 1.67167 \times 10^{-4}*\text{Base concentration} \\
& - 6.83333 \times 10^{-5}*\text{Acrylate mol ratio*Base concentration}
\end{aligned}
$$

(6)

$$
\begin{aligned}
\text{DBU Neat } k_{obs} = {} & -1.55772 \times 10^{-3} + 6.625 \times 10^{-4}*\text{Acrylate mol ratio} \\
& + 1.605 \times 10^{-3}*\text{Base concentration} \\
& - 5.79167 \times 10^{-4}*\text{Acrylate mol ratio*Base concentration}
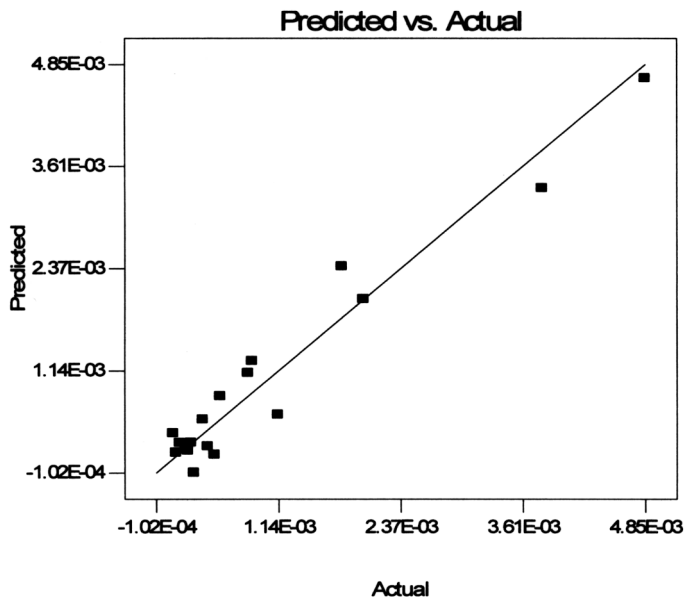\end{aligned}
$$

(7)

Figure 8 The significant relationship between predicted and actual observed rate constants for reactions conducted in the presence of DBU.

From these equations and actual observed rate constants measured from *in-situ* FTIR experiments, a plot of predicted versus actual observed rate constants was constructed, as depicted in Figure 8. Each experimental rate constant is represented by a square. The statistical design model shows a good agreement between predicted and actual observed rate constants.

The effects of each of the factors on the observed rate constants are depicted in Figures 9–11 for reactions conducted in the presence of DBU. The observed rate constant was the smallest for the $0.8 : 1.0$ acrylate to acetoacetate molar ratio and varied for the other molar ratios (Figure 9). Increasing the base concentration and conducting the reactions in solvent-free conditions resulted in greater observed rate constants, as depicted in Figures 10 and 11, respectively.

Contour plots, shown in Figure 12, demonstrate the effect of base concentration and acrylate : AcAc molar ratios on the actual observed rate constants for reactions conducted in the presence of DBU. Figure 12a represents reactions in THF, and Figure 12b represents reactions in solvent-free conditions. A wider range of observed rate constants were achieved in the absence of solvent.
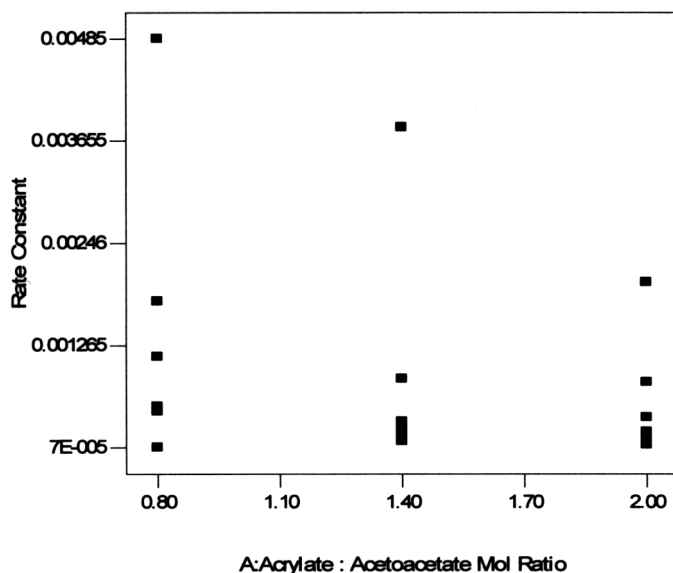
Figure 9 The relationship between acrylate molar ratios and actual observed rate constants for reactions conducted in the presence of DBU.

To optimize observed rate constants above $5 \times 10^{-4}\,s^{-1}$, an overlay plot was constructed. As depicted in Figure 13, to achieve a rate constant of at least $5 \times 10^{-4}\,s^{-1}$, one must use reaction conditions in such a manner that the base
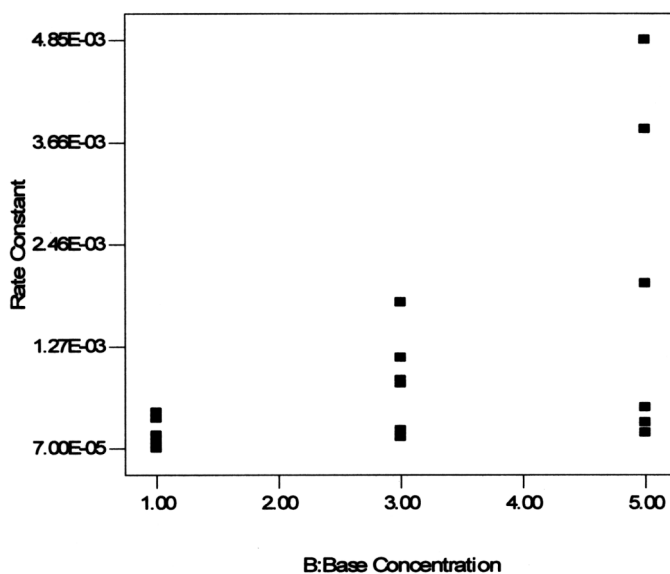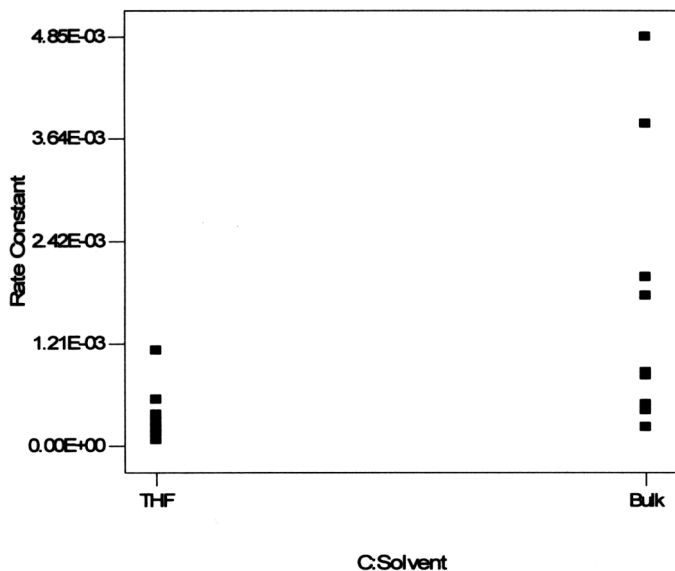

Figure 10 The significant relationship between base concentration and actual observed rate constants for reactions conducted in the presence of DBU.

Figure 11 The significant relationship between the presence of solvent and actual observed rate constants for reactions conducted in the presence of DBU.

concentration and acrylate : AcAc molar ratio are within the shaded area of the graph. Since the rates of reaction are faster in the absence of solvent, there is a greater shaded area for the reaction performed in solvent-free conditions. Figure 13a represents reactions in THF, and Figure 13b represents reactions in solvent-free conditions.
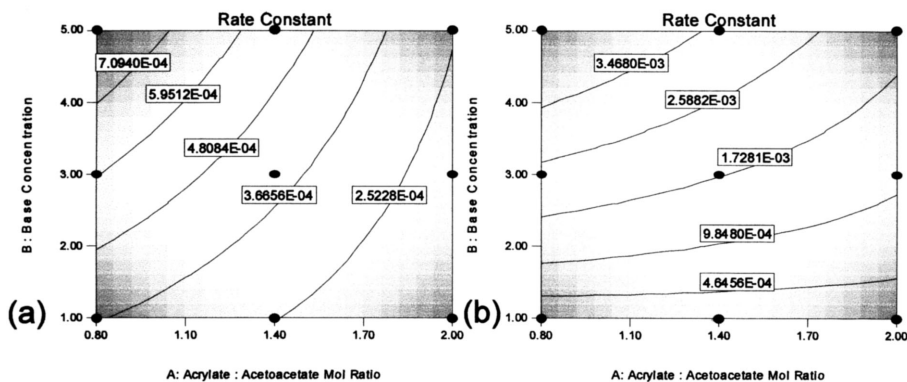
Figure 12 Contour plots of the effect of base concentration and acrylate molar ratios on the actual observed rate constants for reactions conducted in the presence of DBU. (**a**) Reactions in THF; (**b**) reactions in solvent-free conditions.
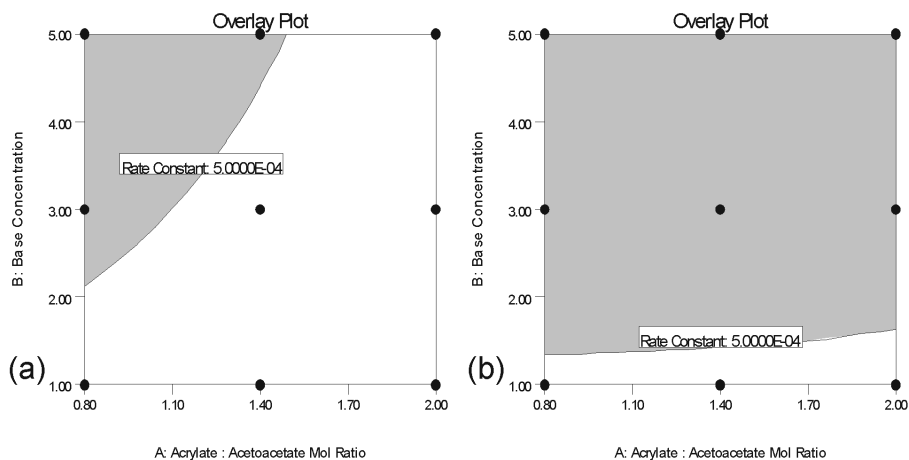
Figure 13   Overlay plots of the effect of base concentration and acrylate molar ratios on the predicted observed rate constants for reactions conducted in the presence of DBU. **(a)** Reactions in THF; **(b)** reactions in solvent-free conditions.

A similar DOE was prepared and analyzed for reactions conducted in the presence of K_2CO_3. The equations in terms of the factors in the presence of K_2CO_3 are:

$$K_2CO_3 \text{ THF } k_{obs} = 5.79132 \times 10^{-5} + 1.06519 \times 10^{-4}*\text{Acrylate mol ratio}$$
$$+ 2.43935 \times 10^{-4}*\text{Base concentration}$$
$$- 8.91017 \times 10^{-5}*\text{Acrylate mol ratio}*\text{Base concentration}$$

$$(8)$$

$$K_2CO_3 \text{ Neat } k_{obs} = -9.05646 \times 10^{-4} + 6.58163 \times 10^{-4}*\text{Acrylate mol ratio}$$
$$+ 1.22873 \times 10^{-3}*\text{Base concentration}$$
$$- 4.89694 \times 10^{-4}*\text{Acrylate mol ratio}*\text{Base concentration}$$

$$(9)$$

In a similar manner to the above, from these equations and actual observed rate constants measured from *in-situ* FTIR experiments, a plot of predicted versus actual observed rate constants was constructed, as depicted in Figure 14. The statistical design model shows a close agreement between predicted and actual observed rate constants. The model did not predict any outlying observed rate constants.
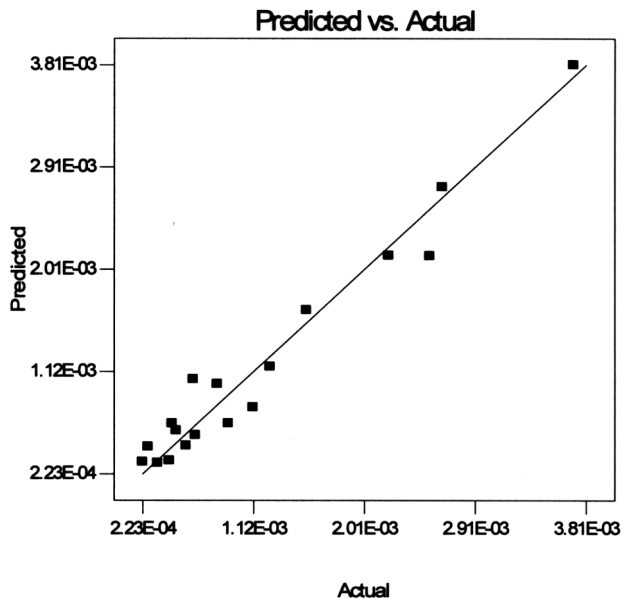
Figure 14 The significant relationship between predicted and actual observed rate constants for reactions conducted in the presence of K_2CO_3.
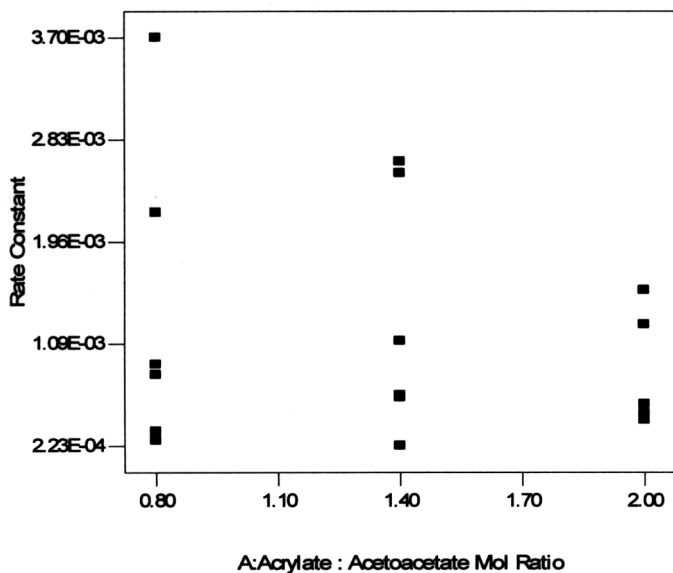

Figure 15 The relationship between acrylate molar ratios and actual observed rate constants for reactions conducted in the presence of K_2CO_3.
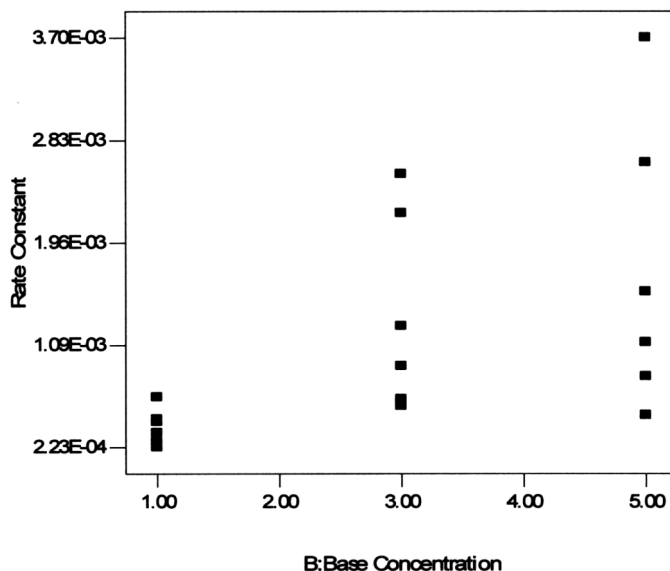
Figure 16 The significant relationship between base concentration and actual observed rate constants for reactions conducted in the presence of K_2CO_3.

The effect of each of the factors on the observed rate constants are depicted in Figures 15 – 17 for reactions conducted in the presence of K_2CO_3. In a similar fashion to reactions conducted in the presence of DBU, the observed rate constant was the smallest for the 0.8 : 1.0 acrylate to acetoacetate molar ratio and varied for the other molar ratios (Figure 15). Increasing the base concentration and conducting the reactions without solvent resulted in greater observed rate constants, as depicted in Figures 16 and 17, respectively.

Contour plots, shown in Figure 18, demonstrate the effect of base concentration and acrylate molar ratios on the actual observed rate constants for reactions conducted in the presence of K_2CO_3. Figure 18a represents reactions in THF, and Figure 18b represents reactions in solvent-free conditions. A wider range of observed rate constants are achieved in solvent-free reaction conditions.

To predict observed rate constants in the presence of K_2CO_3, an overlay plot was constructed. As depicted in Figure 19, to achieve a rate constant of at least $9 \times 10^{-4}\,s^{-1}$, one must use reaction conditions in such a manner that the base concentration and acrylate molar ratio are within the shaded area of the graph. Since the rates of reaction are faster in the absence of solvent, there is a greater shaded area for the reaction performed in neat conditions. The plot on
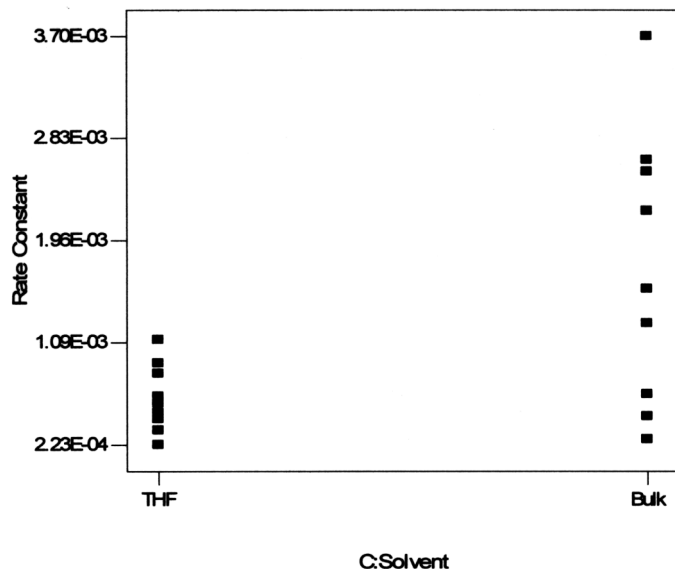
Figure 17   The significant relationship between the presence of solvent and actual
                observed rate constants for reactions conducted in the presence of K_2CO_3.

the left (a) represents reactions in THF, and the plot on the right (b) represents
reactions in solvent-free conditions.

   Of several factors, the presence of solvent and base concentration
contributed the greatest to the observed rate constant. Overall, the greater
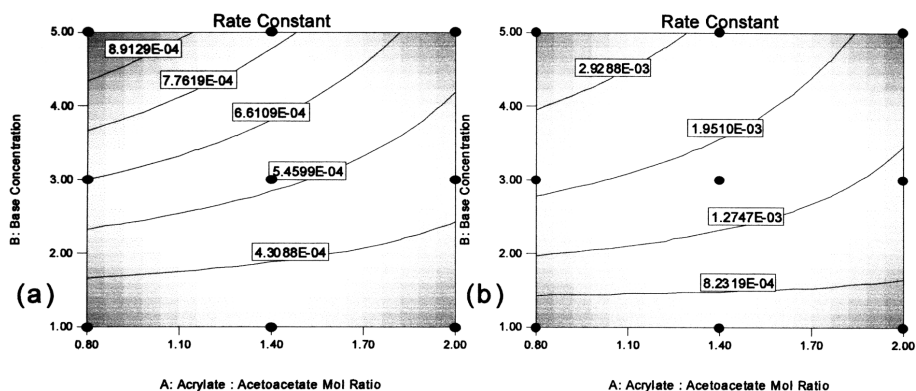observed rate constants were seen when DBU was used as the base.

Figure 18   Contour plots of the effect of base concentration and acrylate molar ratios on
                the actual observed rate constants for reactions conducted in the presence of
                K_2CO_3. **(a)** Reactions in THF; **(b)** reactions in solvent-free conditions.
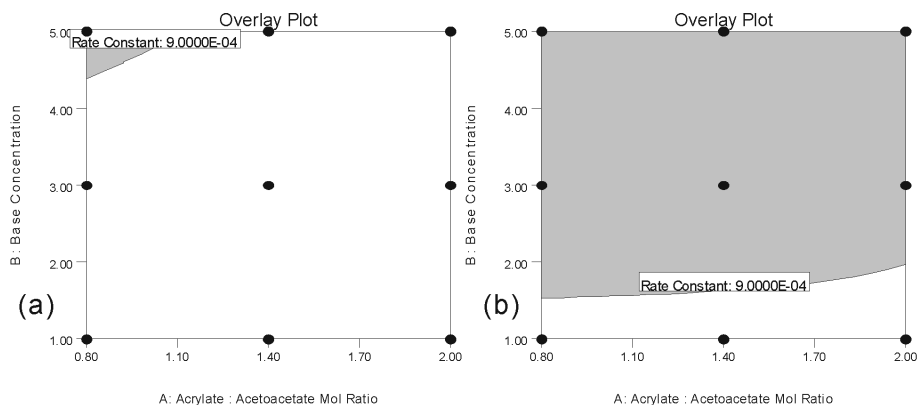
Figure 19 Overlay plots of the effect of base concentration and acrylate molar ratios on the predicted observed rate constants for reactions conducted in the presence of K_2CO_3. (**a**) Reactions in THF; (**b**) reactions in solvent-free conditions.

3.6 Network formation

A series of networks were synthesized from PPG BisAcAc and PPGDA, using DBU or K_2CO_3 as the basic catalyst. The molecular weight of the PPGDA was 800 g/mol, and the molecular weights of the PPG BisAcAc ranged from 1000 to 8000 g/mol. A total of eight different networks were prepared.
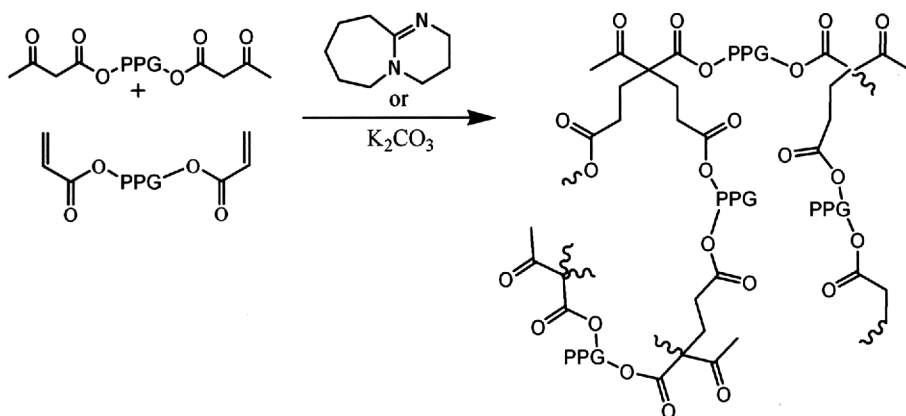
Scheme 4 Network formation via the Michael reaction of PPG BisAcAc and PPGDA.

In a similar fashion to the model studies, *in-situ* FTIR spectroscopy was used to observe the change in the vinyl stretch frequency over the reaction period for each network. The absorbance profiles versus time in seconds are demonstrated in Figures 20 and 21 for networks prepared in the presence of DBU and K_2CO_3,
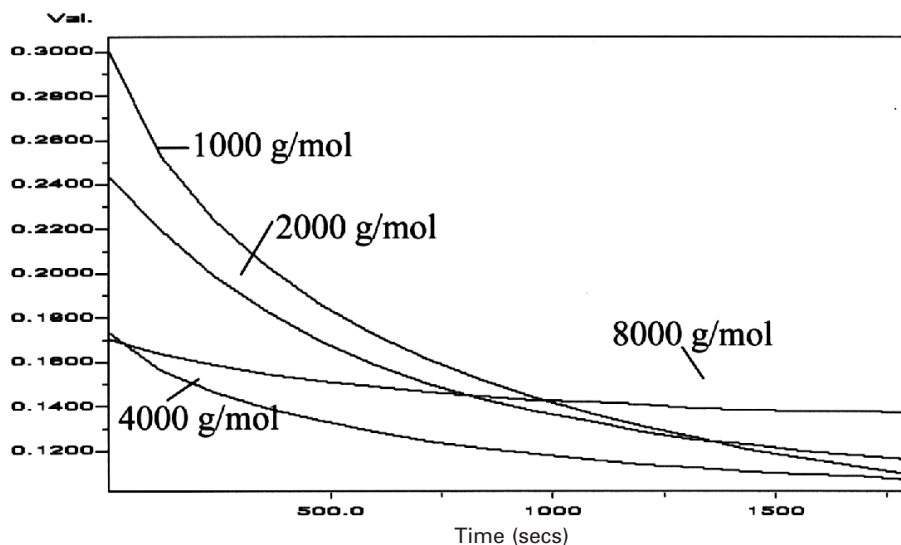
Figure 20   *In-situ* FTIR profiles demonstrating decrease in absorption over time for PPG BisAcAc – PPGDA networks prepared with DBU as the base.
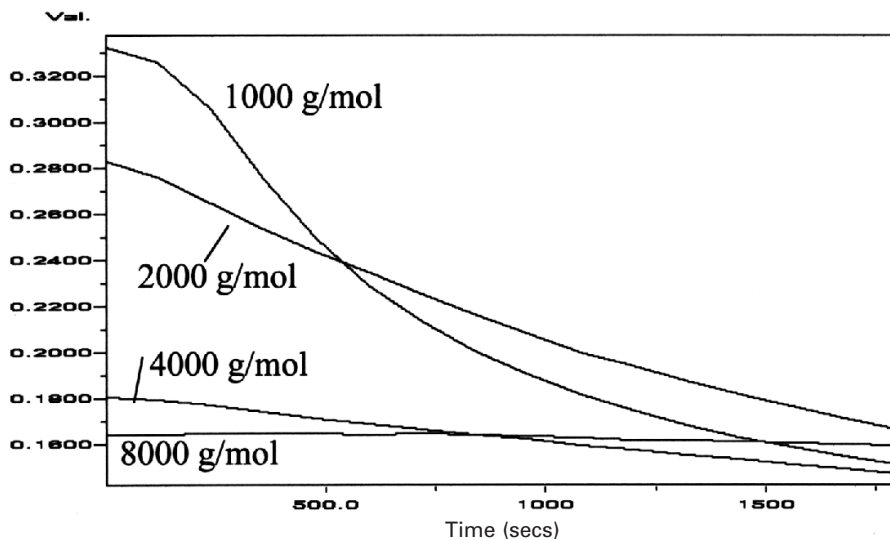

Figure 21   *In-situ* FTIR profiles demonstrating decrease in absorption over time for PPG BisAcAc – PPGDA networks prepared with K_2CO_3 as the base.
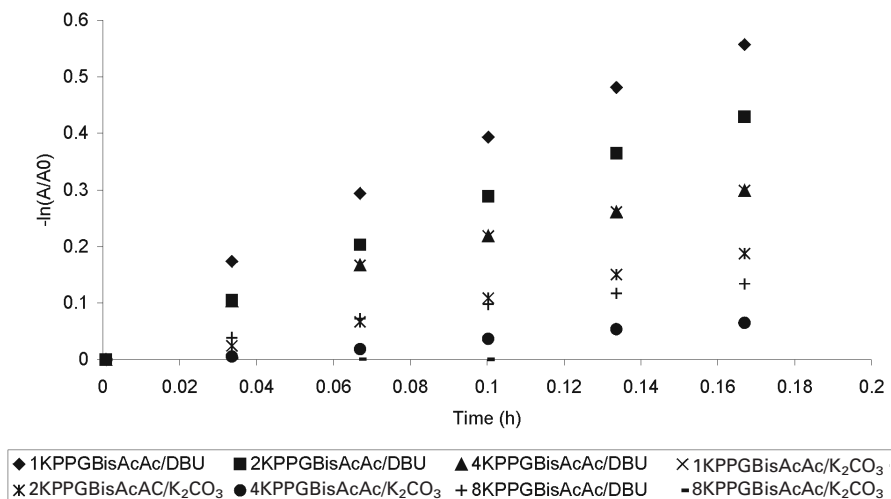
Figure 22   Kinetic plot of PPG BisAcAc – PPGDA network formation.

respectively. As the molecular weight of the PPG BisAcAc segment increased from 1000 g/mol to 8000 g/mol, the change in the intensity of the absorbance profile was not as pronounced, indicating slower reaction rates due to decreased reactive chain end concentration. Furthermore, the decrease in absorbance was not as pronounced for networks prepared with K_2CO_3 as the base.

From the profiles shown in Figures 20 and 21, kinetic plots were constructed and are shown in Figure 22. As the molecular weight of the PPG BisAcAc segment increased, the rate of the reaction decreased. In addition, the rate of the reaction was considerably slower for the networks prepared with K_2CO_3 as the basic catalyst, than with the networks prepared with DBU. The observed rate constants were calculated from the plots and are summarized in Table 4.

Table 4   Observed rate constants from *in-situ* FTIR experiments for PPG BisAcAc – PPGDA network formation

Polymer	Base	k_{obs} (s^{-1})
1000 g/mol PPG BisAcAc – PPGDA	DBU	9.08×10^{-4}
2000 g/mol PPG BisAcAc – PPGDA	DBU	7.18×10^{-4}
4000 g/mol PPG BisAcAc – PPGDA	DBU	4.81×10^{-4}
8000 g/mol PPG BisAcAc – PPGDA	DBU	2.22×10^{-4}
1000 g/mol PPG BisAcAc – PPGDA	K_2CO_3	4.81×10^{-4}
2000 g/mol PPG BisAcAc – PPGDA	K_2CO_3	3.24×10^{-4}
4000 g/mol PPG BisAcAc – PPGDA	K_2CO_3	1.17×10^{-4}
8000 g/mol PPG BisAcAc – PPGDA	K_2CO_3	2.23×10^{-5}

Table 5 Gel time analysis for PPG BisAcAc – PPGDA networks as determined from rheology experiments. The gel time was recorded when $G' = G''$

Polymer	Base	Gel time (s)
1000 g/mol PPG BisAcAc – PPGDA	DBU	243
2000 g/mol PPG BisAcAc – PPGDA	DBU	414
4000 g/mol PPG BisAcAc – PPGDA	DBU	932
8000 g/mol PPG BisAcAc – PPGDA	DBU	1925
1000 g/mol PPG BisAcAc – PPGDA	K_2CO_3	1422
2000 g/mol PPG BisAcAc – PPGDA	K_2CO_3	1525
4000 g/mol PPG BisAcAc – PPGDA	K_2CO_3	1735
8000 g/mol PPG BisAcAc – PPGDA	K_2CO_3	6530

To determine the precise gel point, rheological experiments were conducted. Rheology revealed a dependence of PPG BisAcAc molecular weight on the gel time, as observed from the crossover point of the storage modulus (G') and loss modulus (G''). The gel point increased as the molecular weight of the PPG BisAcAc segment increased. Considerably longer gel times were observed for the networks prepared with heterogeneous base, K_2CO_3. The result of the gel point analysis is shown in Table 5.

Films were prepared in Teflon™ moulds for gel fraction mechanical property analysis. Soxhlet extractions were performed in THF for 3 h. The results are demonstrated in Table 6. All networks were highly cross-linked, with the exception of the networks prepared with 8000 g/mol PPGBisAcAc. As the distance between cross-link points increased and concentration of functional end-groups decreased, the gel fraction decreased. We hypothesized that the use

Table 6 Gel fraction analysis for PPG BisAcAc – PPGDA networks as determined from Soxhlet extractions

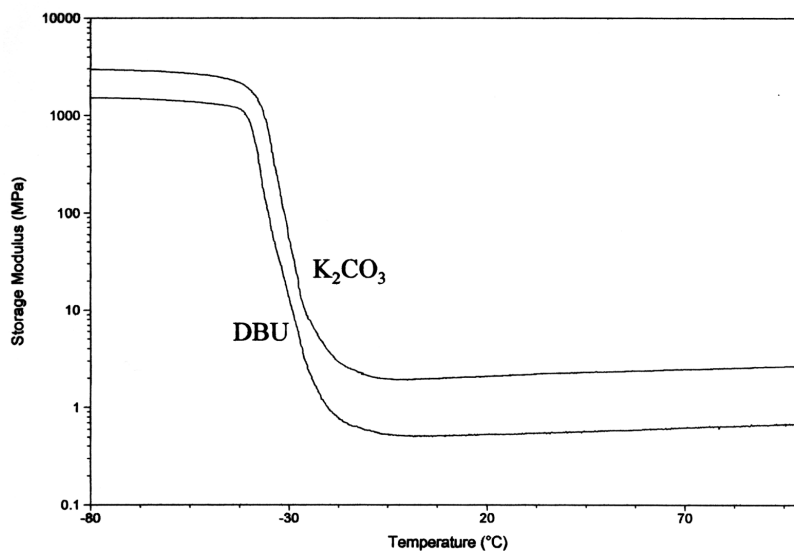| Polymer	Base	Gel fraction (%) ($\pm 2\%$)
1000 g/mol PPG BisAcAc – PPGDA	DBU	93
2000 g/mol PPG BisAcAc – PPGDA	DBU	91
4000 g/mol PPG BisAcAc – PPGDA	DBU	88
8000 g/mol PPG BisAcAc – PPGDA	DBU	71
1000 g/mol PPG BisAcAc – PPGDA	K_2CO_3	97
2000 g/mol PPG BisAcAc – PPGDA	K_2CO_3	96
4000 g/mol PPG BisAcAc – PPGDA	K_2CO_3	92
8000 g/mol PPG BisAcAc – PPGDA	K_2CO_3	72

Figure 23 Storage modulus versus temperature for 1000 g/mol PPG BisAcAc – PPGDA networks.

of inorganic, insoluble, heterogeneous K_2CO_3 would result in lower gel fractions. However, as shown in Table 3, the gel fraction analyses for the two sets of networks were quite similar.
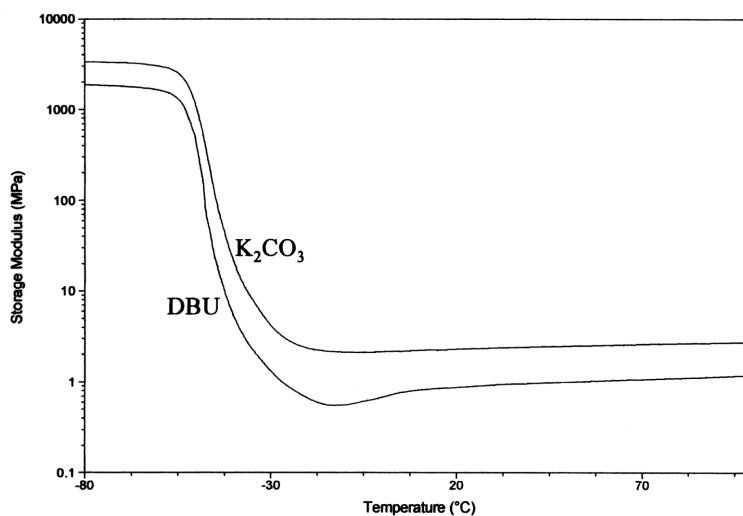

Figure 24 Storage modulus versus temperature for 2000 g/mol PPG BisAcAc – PPGDA networks.

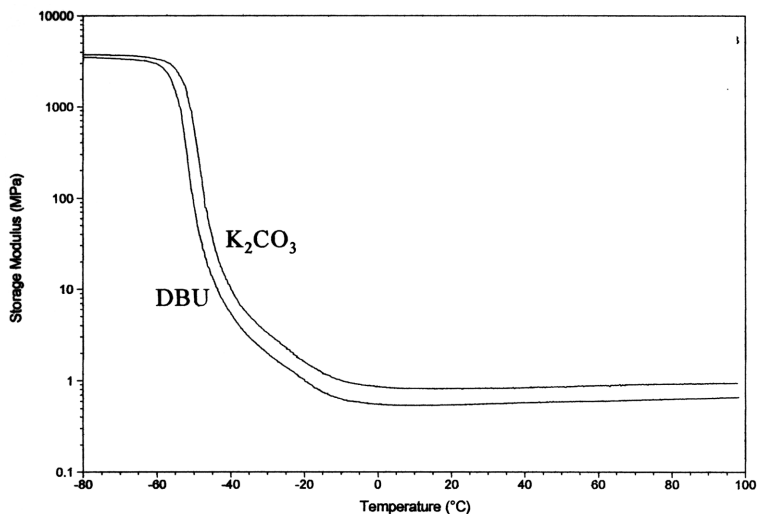*Sharlene R. Williams, Kevin M. Miller and Timothy E. Long*

Figure 25 Storage modulus versus temperature for 4000 g/mol PPG BisAcAc – PPGDA
networks.

The mechanical properties were also very similar for matching molecular
weight sets of networks with either DBU or K_2CO_3 as the base, as shown in
Figures 23 – 26. DMA also revealed a molecular weight dependence as well.
Increasing T_g was observed as the molecular weight of the PPG BisAcAc
segment decreased. Furthermore, as the crosslink density increased, the
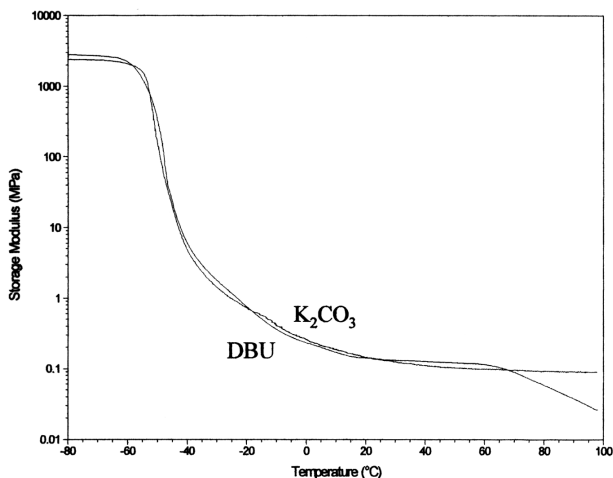modulus of the rubbery plateau increased.

Figure 26 Storage modulus versus temperature for 8000 g/mol PPG BisAcAc – PPGDA
networks.

4. CONCLUSIONS

Model Michael addition reactions were conducted with EHA and EtAcAc to determine the effects of solvent, base, base concentration, and reactant molar ratio on the observed rate constant. The observed rate constants were determined via *in-situ* FTIR. A DOE analysis was conducted for small-molecule Michael reactions prepared with DBU and K_2CO_3 as the base. Cross-linked films were then prepared from PPG BisAcAc and PPGDA in the presence of DBU and K_2CO_3. These networks were prepared in the absence of solvent at 23°C, without the formation of by-products. Network formation was monitored *via in-situ* FTIR, and observed rate constants were calculated. As the molecular weight of the PPG BisAcAc segment increased, the observed rate constant decreased. The influence on PPG BisAcAc molecular weight on mechanical properties was determined *via* DMA and gel fraction analysis. A dependence on PPG BisAcAc molecular weight on gel fraction analysis was observed, and revealed that increasing the molecular weight of PPG BisAcAc precursor resulted in lower gel fractions. However, the base did not change the mechanical properties, according to the DMA results. Therefore, it appears that base type is significant for the rate of the reaction, but not for mechanical properties.

5. ACKNOWLEDGEMENTS

6. REFERENCES

[1]   Moy, T. M., Dammann, L. and Loza, R. U.S. Patent 5,945,489, 1999.
[2]   Kim, Y.-B., Kim, H. K., Nishida, H. and Endo, T. *Macromol. Mater. Eng*., 2004, **289**, 923–926.
[3]   Mather, B. D., Miller, K. M. and Long, T. E. *Macromol. Chem. Phys*., 2006, **207**, 1324–1333.

[4]   Mather, B. D., Viswanathan, K. V., Miller, K. M. and Long, T. E. *Prog. Polym. Sci.*, 2006, **31**, 487–531.

[5]   Kauffman, T. F., Whitman, D. W. and Zajackowski, M. J. U.S. Patent Application Number 20060078742, 2006.

[6]   Kauffman, T. F., Whitman, D. M., Zajaczkowski, M. J. and Vietti, D. E. European Patent EP20050255458 20050907, 2006.

[7]   Wang, D., Liu, Y., Hong, C.-Y. and Pan, C.-Y. *Polymer*, 2006, **47**, 3799–3806.

[8]   Rizzi, S. C. and Hubbell, J. A. *Biomacromolec.*, 2005, **6**, 1226–1238.

[9]   Elbert, D. L., Pratt, A. B., Lutolf, M. P., Halstenberg, S. and Hubbell, J. A. *J. Control Release*, 2001, **76**, 11–25.

[10] Lutolf, M. P. and Hubbell, J. A. *Biomacromolec.*, 2003, **4**, 713–722.

[11] Rizzi, S. C., Ehrbar, M., Halstenberg, S., Raeber, G. P., Schmoekel, H. G., Hagenmuller, H., Muller, R., Weber, F. E. and Hubbell, J. A. *Biomacromolec.*, 2006, **7**, 3019–3029.

[12] Albertson, N. F. *J. Am. Chem. Soc.*, 1948, **70**, 669–670.

[13] Schultz, A. G. and Yee, Y. K. *J. Org. Chem.*, 1976, **41**, 4044–4045.

[14] Clemens, R. J. and Rector, F. D. *J. Coat. Technol.*, 1989, **61**, 83–91.

[15] Williams, S. R., Mather, B. D., Miller, K. M. and Long, T. E. *J. Polym. Sci.* (A) *Chem.*, 2007, **45**(17), 4118–4128.

[16] Little, R. D., Masjedizadeh, M. R., Wallquist, O. and McLoughlin, J. I. In: *Organic Reactions*, Wiley, New York, 1995. pp. 315–552.

[17] Jung, M. E. In: *Comprehensive Organic Synthesis*, Pergamon, Oxford, 1991. pp. 1–67.

[18] Bergman, E. D., Ginsburg, D. and Pappo, R. In: *Organic Reactions*, 1959. pp. 179–556.

[19] Carey, F. A. and Sundberg, R. J. *Advanced Organic Chemistry: Part A. Structure and Mechanisms*. Plenum Press, New York, 1999.

[20] Smith, M. B. and March, J. *March's Advanced Organic Chemistry*. Wiley-Interscience, 2001.